

# The twentieth century was the wettest period in northern Pakistan over the past millennium

Kerstin S. Treydte<sup>1</sup>, Gerhard H. Schleser<sup>2</sup>, Gerhard Helle<sup>2</sup>, David C. Frank<sup>1</sup>, Matthias Winiger<sup>3</sup>, Gerald H. Haug<sup>4</sup> & Jan Esper<sup>1</sup>

Twentieth-century warming could lead to increases in the moisture-holding capacity of the atmosphere, altering the hydrological cycle and the characteristics of precipitation<sup>1</sup>. Such changes in the global rate and distribution of precipitation may have a greater direct effect on human well-being and ecosystem dynamics than changes in temperature itself<sup>2,3</sup>. Despite the co-variability of both of these climate variables<sup>3</sup>, attention in long-term climate reconstruction has mainly concentrated on temperature changes<sup>4–8</sup>. Here we present an annually resolved oxygen isotope record from tree-rings, providing a millennial-scale reconstruction of precipitation variability in the high mountains of northern Pakistan. The climatic signal originates mainly from winter precipitation, and is robust over ecologically different sites. Centennial-scale variations reveal dry conditions at the beginning of the past millennium and through the eighteenth and early nineteenth centuries, with precipitation increasing during the late nineteenth and the twentieth centuries to yield the wettest conditions of the past 1,000 years. Comparison with other long-term precipitation reconstructions indicates a large-scale intensification of the hydrological cycle coincident with the onset of industrialization and global warming, and the unprecedented amplitude argues for a human role.

The high mountain systems of Central Asia control atmospheric circulation patterns with stationary low and high pressure systems resulting from heating and cooling interactions with the lower troposphere, respectively<sup>9</sup>. Although there is increasing knowledge about regional temperature trends over the last millennium—showing warmth in Medieval times, cooling during the ‘Little Ice Age’ and recent warming<sup>10,11</sup>—few investigations, restricted primarily to recent centuries and focusing mainly on monsoonal regions<sup>12–17</sup>, address variations in precipitation. However, improving knowledge regarding long-term precipitation changes and potential large-scale

trends is of great importance for future predictions of regional and global hydrological cycles<sup>2</sup>.

Our study sites include the western part of High Asia with the Karakorum and Himalayan mountains in northern Pakistan, surrounding the upper reaches of the Indus Valley and supplying the world’s largest irrigation network. This high mountain system interacts predominantly with westerly synoptic fronts and catalyses the formation of meridional troughs in the jet stream (Rossby waves). The climate is of ‘Mediterranean character’, with precipitation being highly variable during summer and at a maximum during winter and spring, resulting in extensive snow cover.

We have evaluated precipitation changes through four, annually resolved oxygen isotope ratio ( $\delta^{18}\text{O}$ ) chronologies from juniper tree-ring cellulose (*Juniperus excelsa*, *J. turkestanica*). Three of these records cover the twentieth century and one extends back to AD 828. The latter was used to reconstruct precipitation variability over the past millennium.

Our study sites are located in three valleys south and north of the main Karakorum range (Fig. 1). They transect a southwest–northeast precipitation gradient with increasing rain-shadow effects northward through the mountain ranges. Three sites are situated near the upper timberline (>3,700 m above sea level, a.s.l.) and one near the lower timberline (2,900 m). According to local site ecology and vegetation cover classification, two sites were classified as cold/moist (‘Ram’ and ‘Bag-high’), one as warm/dry (‘Bag-low’), and one, containing the >1,000-year-old trees, as cold/dry (‘Mor’). Except for the Mor site,  $\delta^{18}\text{O}$  measurements are confined to the period 1900–1998 (Supplementary Table 1). All sites inter-correlate significantly ( $P < 0.001$ ) (Fig. 2a), suggesting common climatic forcing independent of potentially differing moisture sources, elevation and local ecological conditions. Similarities in the annual series are not limited to the

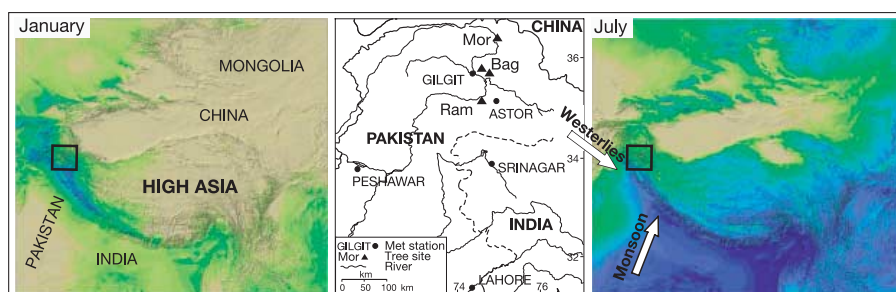


**Figure 1 | Site locations and Central Asian average precipitation distribution<sup>9</sup> in January and July.** The study area is dominated by westerly synoptic fronts throughout the year (dark colours indicate high precipitation levels). ‘Bag’ includes one high (3,900 m a.s.l.) and one low

(2,900 m a.s.l.) elevation site. ‘Mor’ (3,900 m a.s.l.) contains >1,000-year-old living trees. The maps are reprinted from ref. 9 (<http://www.tandf.no/>) with permission from Taylor & Francis.

<sup>1</sup>Swiss Federal Research Institute WSL, Zürcherstrasse 111, CH-8903 Birmensdorf, Switzerland. <sup>2</sup>Forschungszentrum Jülich GmbH, ICG-V, Leo-Brandt-Strasse, D-52425 Jülich, Germany. <sup>3</sup>University of Bonn, Meckenheimer Allee 166, D-53115 Bonn, Germany. <sup>4</sup>GeoForschungszentrum Potsdam, Telegrafenberg, C324, D-14473 Potsdam, Germany.

inter-annual (high-frequency) but also exist on decadal timescales. The range in 1900–1998  $\delta^{18}\text{O}$  mean values (28.6–31.1‰ between sites) is, however, related to absolute levels of local soil moisture availability, and hence to variable transpiration rates and leaf water enrichment<sup>18</sup>.

Correlation analyses using all  $\delta^{18}\text{O}$  site records, their mean and variance-adjusted average (which we term Kara, derived from Karakorum), and regionalized climate data (REG; Supplementary Fig. 1) show no strong link to temperature variations but do correlate significantly with precipitation totals (Fig. 2b and Supplementary Fig. 3). This pattern is common between the sites, and has greatest similarities to mean annual precipitation (measured from the end of the vegetation period from the previous year to the end of the subsequent one: October–September), which is dominated by the winter half-year precipitation from October to March. Hence, tree-ring  $\delta^{18}\text{O}$  serves as a proxy for the amount of precipitation, which at these elevations primarily falls as snow, providing the main source of water for the trees. This holds especially in spring, when early wood cells, which account for about 90% of the total ring width (roughly 80% of ring mass), are formed. The effect persists in part during summer, as much of the summer precipitation at high elevations falls as snow (but contributes less than 20% to the annual total). Snowmelt provides a more stable water source than rainfall with rapid surface runoff, which is supported through slightly positive correlations with summer temperatures. Potential effects of varying ratios of snow and rainfall could also affect the detected climate signal, but were not supported by calibration tests against instrumental data. The detected signal stems largely from the markedly depleted snowfall that dominates the annual precipitation regime<sup>19,20</sup>. The negative relationship between precipitation totals and tree-ring  $\delta^{18}\text{O}$  is strengthened through complex effects of varying humidity on plant physiology<sup>18</sup>. Simplified, moist

atmospheric conditions will reduce transpiration and therefore reduce  $^{18}\text{O}$  water enrichment in needles. When incorporated into organic matter, this results in lower tree-ring  $\delta^{18}\text{O}$  values<sup>18</sup>.

The system of snowfall, melt water supply, soil moisture and transpiration leaves a fingerprint on the  $\delta^{18}\text{O}$  signal in cellulose, leading to an integrated precipitation signal over all seasons.  $\delta^{18}\text{O}$  measurements of Kara, integrating all twentieth-century site chronologies, correlate with the October–September precipitation series (REG) at  $r = 0.58$  (1898–1990,  $P < 0.001$ ). In particular, the decadal-scale variations of increased precipitation (1930s, 1960s) and reduced precipitation are captured quite closely (Fig. 3a). Calibration and verification tests using the 1898–1944 ( $r = 0.49$ ,  $P < 0.001$ ) and 1944–1990 ( $r = 0.69$ ,  $P < 0.001$ ) periods suggest temporal stability of this relationship, despite the reduced replication, spatial representativity and lower quality of early instrumental data. Correlations using only Mor data are highly significant but slightly reduced, with  $r$  values of 0.42 and 0.62 over the 1898–1944 and 1944–1990 periods, respectively, indicating that increased signal quality is obtained with greater numbers of sites. Verification tests using reduction of error (RE) and coefficient of efficiency (CE) statistics<sup>21</sup> yielded 0.36 (RE) and 0.24 (CE) for the recent (1944–1990), and 0.14 (RE) and  $-0.03$  (CE) for the early (1898–1944) verification periods, indicating high reconstruction quality.

We addressed reconstruction complications due to possible age effects in the record by indicating deviations from the reconstruction using all data (shown in black in Fig. 3b) compared to reconstruction using only tree-ring data from biologically old rings during the 1264–1599 and 1010–1179 periods (red in Fig. 3b). We find that potential age-related biases, as reported for reconstructions based on ring width<sup>5</sup>, only slightly affect long-term climate reconstructions using  $\delta^{18}\text{O}$  measurements. The peak values reconstructed for the 1350s and 1470s using only juvenile tree-rings are higher relative

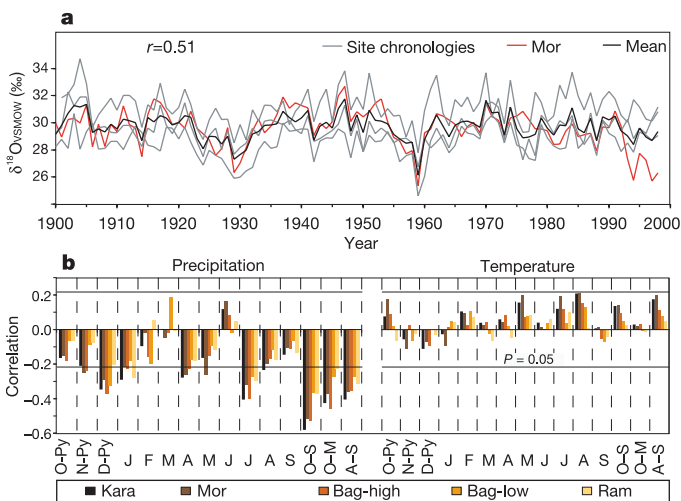


**Figure 2** |  $\delta^{18}\text{O}$  site chronologies and climate correlation. **a**, Site chronologies, including the most recent part of the millennial-long Mor record, together with the grand mean of all sites.  $r$  is the mean inter-series correlation.  $\delta^{18}\text{O} = [((^{18}\text{O}/^{16}\text{O})_{\text{sample}} / (^{18}\text{O}/^{16}\text{O})_{\text{standard}}) - 1] \times 1,000$ . **b**, Correlations between regionalized precipitation and temperature records (REG), the  $\delta^{18}\text{O}$  site records, and the adjusted average, 'Kara'. REG was calculated by averaging station anomalies for temperature, and normalized indices for precipitation. Kara is the arithmetic mean of the site records, after adjusting the twentieth-century mean  $\delta^{18}\text{O}$  values and their variance to Mor. Climate correlations are calculated for individual months from October of the previous year ('O-Py') to September of the following year ('S'), their mean ('O-S'), winter half-year (October–March, 'O-M') and summer half-year (April–September, 'A-S'). Correlations cover the full period of instrumental station data with a minimum replication  $> 2$  (AD 1898–1990) (Supplementary Figs 1, 3). 95% significance levels are adjusted for lag  $- 1$  autocorrelation.

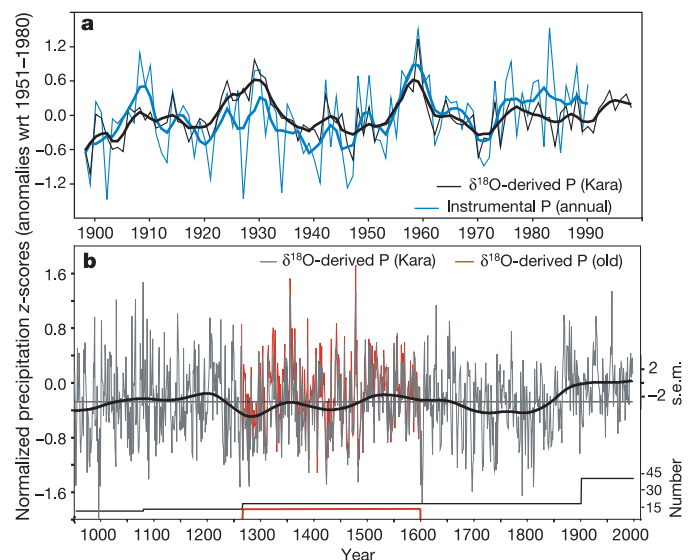


**Figure 3** |  $\delta^{18}\text{O}$ -derived precipitation reconstruction for northern Pakistan. **a**, Annual precipitation values (1898–1990) of instrumental and modelled data with respect to (wrt) the 1951–1980 mean. Smoothed curves are 5-year Kernel filters. **b**, Precipitation reconstruction using all tree-ring data (Kara) since AD 950. Proxy data were calibrated using a linear regression (1898–1990). Note that the raw  $\delta^{18}\text{O}$  record is inverted here owing to the negative sign of the regression slope (Supplementary Fig. 4). The horizontal line is the overall mean of the reconstruction. For the period 1264–1599, maximum deviations are in red when using data from only old tree-rings (Supplementary Fig. 4 and Supplementary Notes). Replication of the reconstruction is three trees (6 cores) in AD 950. Long-term variations are highlighted using a 150-year spline. Uncertainty estimates for the low-frequency domain are indicated by two standard errors (see Methods).

to the continuous record integrating all data. Nonetheless, this age-related bias does not change the overall centennial-scale (low-frequency) pattern of reconstructed precipitation (Supplementary Fig. 4 and Supplementary Notes).

Our precipitation reconstruction over a millennium (Fig. 3b) reveals a cluster of peak precipitation periods during the late nineteenth and the twentieth century that are towards the upper limit of the distribution reconstructed over the past 1,000 years, with the majority of values before the twentieth century falling below the 1951–1980 mean. Wet periods of decadal length occur around 1200, 1350, 1500 and 1870; and dry periods occur before 1000 and around 1270, 1420, 1600 and 1720. The dry 1790s and 1890s are known as periods of severe famines in India<sup>12</sup>. Tree-ring reconstructions from across High Asia confirm particularly intensified pluvial conditions in the twentieth century in India<sup>13,14</sup>, Mongolia<sup>15</sup> and Tibet<sup>16</sup>.

The spectral characteristics of the millennium-long  $\delta^{18}\text{O}$ -derived precipitation reconstruction (Supplementary Fig. 5) show more low-frequency loading than is commonly reported for observational precipitation data<sup>22</sup>. This lower-frequency variation over the past

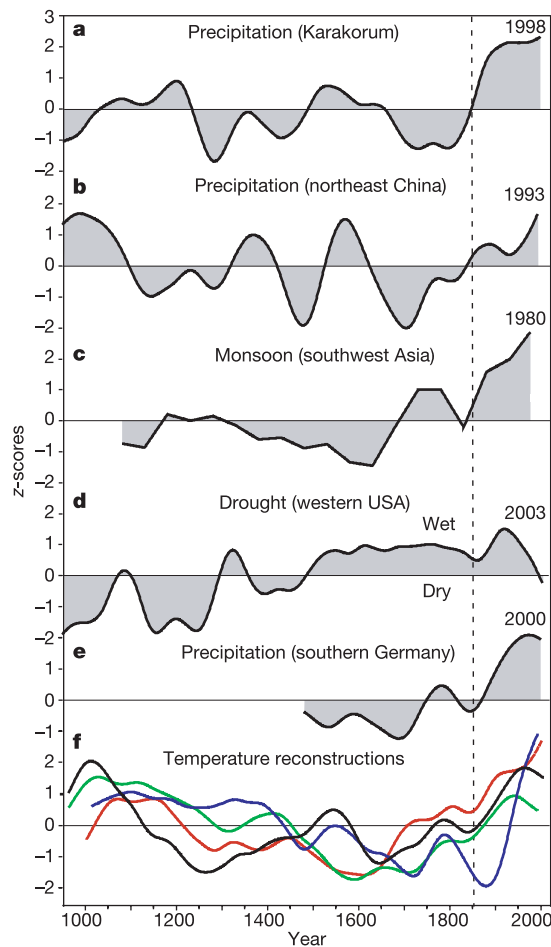


**Figure 4 | Precipitation reconstruction for northern Pakistan and long-term precipitation variations for different regions in the northern hemisphere.** **a**, Tree-ring  $\delta^{18}\text{O}$ -derived reconstruction. **b**, Annual precipitation reconstruction (July–June) from tree-rings in northeast China<sup>17</sup>. **c**, Southwest Asian monsoon intensity from *Globigerina bulloids* in the Arabian sea<sup>12</sup>. **d**, Drought reconstruction from tree rings in western USA<sup>23</sup>. **e**, Spring–summer precipitation reconstruction from tree-rings in southern Germany<sup>24</sup>. **f**, Regional to hemispheric temperature variations according to ref. 11 (red, western Central Asia), ref. 4 (blue), ref. 5 (black) and ref. 8 (green). Records are normalized over their individual periods and smoothed using 150-year splines. Numbers in **a–e** refer to the last year of the records, and the black dashed line to the shift from negative to positive precipitation anomalies in the Karakorum record.

1,000 years has trends similar to those found in long-term precipitation and drought reconstructions from synoptically different regions. Figure 4 shows the low-frequency components of our precipitation record (Fig. 4a) together with recently developed long-term precipitation reconstructions from semi-arid northeast China<sup>17</sup>, monsoonal southwest Asia<sup>12</sup>, the western United States<sup>23</sup> and Germany<sup>24</sup>. As these reconstructions represent rather different atmospheric circulation regimes, and considering that precipitation variations are spatially and temporally more heterogeneous than temperature variations, it is not surprising that these time series do not correlate on annual-to-decadal scales. However, for the lowest-frequency component, there is evidence for a large-scale trend towards pluvial conditions in the twentieth century, particularly in Eurasian reconstructions (Fig. 4). In the western United States, the recent trend in the second half of the twentieth century indicates a change towards drier conditions, related to Pacific sea surface temperature and El Niño/Southern Oscillation dynamics<sup>23</sup>. Nevertheless, the overall long-term trend towards pluvial conditions in all records is consistent with a regional-to-large-scale temperature increase over the past 150 years<sup>4,5,8,11</sup> (Fig. 4f), which is itself described to be at least partly forced by the increase in anthropogenic greenhouse gases during this time<sup>25</sup>.

Globally observed annual precipitation trends indicate a twentieth-century increase of 9 mm over land areas, which is approximately 0.98% per decade<sup>22</sup>. There is evidence that warming leads to increases in the moisture-holding capacity of the atmosphere at a rate of about 7%  $\text{K}^{-1}$ , altering the hydrological cycle and characteristics of precipitation events, including their amount, frequency, intensity and duration. Depending on the feedback mechanisms included, similar or slightly larger increases are estimated for rainfall intensity<sup>1</sup>. However, best estimates for total rainfall increases are smaller, falling within the range of  $\sim 1.0$ –3.4%  $\text{K}^{-1}$  (refs 2, 26). These differences suggest interplay between rainfall characteristics and the dependence of precipitation totals on total available energy, which is decreased by the increased ability of the troposphere to radiate away latent heat released by precipitation<sup>1</sup>. A compilation of coupled ocean–atmosphere and atmosphere-only model runs shows that precipitation decreases at subtropical latitudes, and increases at high latitudes, around the Equator and across much of Asia, consistent with the evidence presented here. Overall, a 6% increase in global mean precipitation between the 1981–2000 and 2081–2100 periods is predicted from these models<sup>27</sup>.

The controls on past and future precipitation patterns and levels are certainly not exclusively related to temperature, but reflect complex circulation and thermodynamic effects with great regional and temporal variations. Nevertheless, our study identifies large-scale similarities in precipitation variation on centennial timescales despite dissimilarity in the higher-frequency domain. We suggest that an unprecedented twentieth-century intensification of the hydrological cycle in western Central Asia has already occurred. It seems that this finding is not only restricted to summer conditions and monsoonal regions, but rather is of a broader seasonal and spatial extent. Moreover, the structure of our record suggests that this climatic change is not simply a temporary fluctuation, but rather a secular trend. If this change were brought about by anthropogenic forcing of climate, as seems most plausible, then further changes can be expected in the near future, and high- and lowland ecological and economic systems in Pakistan and India will be forced to adapt.

## METHODS

**Sample preparation.** Our sampling strategy was based on considering only sites with steep slopes ( $>35^\circ$ ) and trees growing in shallow and well-drained soils, to minimize potential effects of long-standing, depleted soil and ground water. The sampling design in high-elevation environments greatly amplifies the influence of melt water on the tree-ring  $\delta^{18}\text{O}$  signal. This influence dominates over other potential signals, such as temperature-dependent fractionation effects that are not found in the Karakorum junipers.

At all sites 12 to 20 trees were sampled, with four cores taken per tree. Ring widths were measured using a semi-automated RinnTech system with a

resolution of 0.01 mm, crossdated using standard procedures, and 5–7 trees per site (two cores per tree) were chosen for isotope analysis. Criteria for sample selection were low numbers of missing rings and regular ring boundaries. To facilitate analysis, we pooled most of the tree-ring material before cellulose extraction. At the Mor site, 14 cores from seven trees were pooled to reach back to AD 828. At the other sites, we pooled tree-rings from 4–5 trees<sup>28</sup>. Single-tree measurements were also undertaken during selected periods. Signal strength analysis using the ‘expressed population signal’ (EPS)<sup>29</sup> indicates that a minimum of 3.5 series would be satisfactory to develop a (population-) representative site record, capturing 85% of the variance of the theoretical, infinite population chronology.

Tree-rings were separated with a scalpel and samples were ground using an ultracentrifugal mill (Retsch ZM1). Cellulose was extracted and cellulose samples (250 µg) were pyrolyzed to CO at 1,080 °C using a Carlo Erba 1500 elemental analyser (CE Instruments) interfaced with an Optima IRMS (Micromass Ltd). δ<sup>18</sup>O values are referenced to Vienna standard mean ocean water (VSMOW). Overall analytical precision, estimated from periodic standard deviation calculations using a commercial cellulose standard (FLUKA), is ±0.3‰.

**Meteorological data setup.** We screened monthly and seasonal temperature and precipitation data for 30 meteorological stations. Five stations were selected for calibration purposes based on the distance to the tree sites, number of missing values, and homogeneity and period of measurements. Two of these stations, Gilgit (GIL, 1,460 m a.s.l.) and Astor (AST, 2,166 m a.s.l.), are located in the study region near the tree sites (Fig. 1), but their records are rather short (GIL = 48 years, AST = 36 years). Srinagar (SRI, 1,587 m a.s.l.), is the closest station with data spanning more than 100 years (AD 1898–1998), and correlates significantly with GIL and AST. The Peshawar (PES, 360 m a.s.l., AD 1864–1990) and Lahore stations (LAH, 214 m a.s.l., 1864–1990), located at a greater distance to the tree sites but have data for >100 years, correlate weakly with the inner-mountainous stations GIL and AST but significantly with SRI. PES and LAH were therefore used for better replication and to reinforce regional climate conditions, particularly in the early period (Supplementary Table 2).

For the development of a regional mean record (REG), temperature means were calculated by averaging monthly anomalies with respect to the 1951–1980 mean. To minimize the effect of significantly differing means and variances, regional precipitation means were calculated by averaging standardized values; that is, monthly data were normalized with respect to the lengths of individual station measurements (Supplementary Fig. 1). These z-scores were not converted back to ‘absolute’ values, because of the dependence of precipitation totals on elevation, making the choice of an ‘absolute’ rainfall level rather arbitrary. The 1898–1990 interval, which is covered by at least two stations, was used for calibration.

**Uncertainty estimation.** For the long reconstruction, 95% confidence intervals for the annual scale were estimated using twice the r.m.s. error derived from a ‘leave-one-out’ cross-validation over the entire 1898–1990 instrumental period (2 s.e.m. = 1.17). Confidence limits based on the r.m.s.e. of the verification data from the split period calibration/verification trials were similar, although about 1% and 10% larger for the early and late verification period data, respectively, demonstrating the benefit of using more data for model calibration. Some additional uncertainty in the reconstruction model may be related to poor early instrumental records and uncertainty in the statistical model definition due to a necessarily limited calibration interval. The short instrumental period does not allow for calibration/verification of centennial-scale variability. As no direct statistical calibration of centennial-scale variability is possible, the regression model is assumed to be frequency-independent. However, we estimated the standard error for the smoothed data by multiplying the square root of the unexplained variance by the standard deviation of the target instrumental data (2 s.e.m. = 0.22). At these wavelengths, this calculation results in a more conservative estimate than the methods for timescale-dependent error bars described earlier<sup>30</sup>. Note that these confidence limits do not consider declines in the proxy quality back in time or potential age-trends in the isotope data, and assume the relationship between the proxy and instrumental data to be temporally stable. The standard error in Fig. 3 is expressed relative to the 1898–1998 mean.

Received 22 August 2005; accepted 23 March 2006.

1. Trenberth, K. E., Dai, A., Rasmussen, R. M. & Parsons, D. B. The changing character of precipitation. *Bull. Am. Meteorol. Soc.* **84**, 1205–1217 (2003).
2. Intergovernmental Panel on Climate Change, *Climate Change 2001: The Scientific Basis* (IPCC, Geneva, 2001).
3. Trenberth, K. E. & Shea, D. J. Relationships between precipitation and surface temperature. *Geophys. Res. Lett.* **32**, 10.1029/2005GL022760 (2005).
4. Mann, M. E., Bradley, R. S. & Hughes, M. K. Northern Hemisphere temperatures during the past millennium: Inferences, uncertainties, and limitations. *Geophys. Res. Lett.* **26**, 759–762 (1999).
5. Esper, J., Cook, E. R. & Schweingruber, F. H. Low-frequency signals in long

chronologies for reconstructing past temperature variability. *Science* **295**, 2250–2253 (2002).

6. Briffa, K. R. & Osborn, T. J. Blowing hot and cold. *Science* **295**, 2227–2228 (2002).
7. Esper, J., Frank, D. C. & Wilson, R. J. S. Climate reconstructions: Low-frequency ambition and high-frequency ratification. *Eos* **85**, 113–119 (2004).
8. Moberg, A., Sonechkin, D. M., Holmgren, K., Datsenko, N. M. & Karlen, W. Highly variable Northern Hemisphere temperatures reconstructed from low- and high-resolution proxy data. *Nature* **433**, 613–617 (2005).
9. Boehner, J. General climatic controls and topoclimatic variations in Central and High Asia. *Boreas* (in the press).
10. Bao, Y., Braeuning, A., Johnson, K. R. & Yafeng, S. General characteristics of temperature variation in China during the last two millennia. *Geophys. Res. Lett.* **29**, 10.1029/2001GL014485 (2002).
11. Esper, J., Frank, D. C., Wilson, R. J. S., Büntgen, U. & Treydte, K. Uniform growth behavior among central Asian low and high elevation juniper tree sites. *Mount. Res. Dev.* (in the press).
12. Anderson, D. M., Overpeck, J. T. & Gupta, A. K. Increase in the Asian southwest monsoon during the past four centuries. *Science* **297**, 596–599 (2002).
13. Hughes, M. K. in *Climate Since AD 1500* (eds Bradley, R. S. & Jones, P. D.) 415–431 (Routledge, London, 1995).
14. Singh, J. & Yadav, R. R. Spring precipitation variations over the western Himalaya, India, since AD 1731 as deduced from tree-rings. *J. Geophys. Res.* **110**, 10.1029/2004JD004855 (2005).
15. Pederson, N., Jacoby, G. C., D’Arrigo, R. D., Cook, E. R. & Buckley, B. Hydrometeorological reconstructions for Northeastern Mongolia derived from tree-rings: 1651–1995. *J. Clim.* **14**, 872–881 (2001).
16. Bräuning, A. & Mantwill, B. Summer temperature and summer monsoon history on the Tibetan Plateau during the last 400 years recorded by tree-rings. *Geophys. Res. Lett.* **32**, 10.1029/2004GL020793 (2005).
17. Sheppard, P. R. et al. Annual precipitation since 515 BC reconstructed from living and fossil juniper growth of northeastern Qinghai Province, China. *Clim. Dyn.* **23**, 869–881 (2004).
18. Roden, J. S., Lin, G. & Ehleringer, J. R. A mechanistic model for interpretation of hydrogen and oxygen isotope ratios in tree-ring cellulose. *Geochim. Cosmochim. Acta* **64**, 21–35 (2000).
19. Rozanski, K., Araguas-Araguas, L. & Gonfiantini, R. Relation between long-term trends of oxygen-18 isotope composition of precipitation and climate. *Science* **258**, 981–985 (1992).
20. Tang, K. & Feng, X. The effect of soil hydrology on the oxygen and hydrogen isotopic compositions of plants’ source water. *Earth Planet. Sci. Lett.* **185**, 355–367 (2001).
21. Cook, E. R., Briffa, K. R. & Jones, P. D. Spatial regression methods in dendroclimatology: a review and comparison of two techniques. *Int. J. Climatol.* **14**, 379 (1994).
22. New, M., Todd, M., Hulme, M. & Jones, P. Precipitation measurements and trends in the twentieth century. *Int. J. Climatol.* **21**, 1889–1922 (2001).
23. Cook, E. R., Woodhouse, C., Eakin, C. M., Meko, D. M. & Stahle, D. W. Long-term aridity changes in the western United States. *Science* **306**, 1015–1018 (2004).
24. Wilson, R. J. S., Luckman, B. H. & Esper, J. A 500-year dendroclimatic reconstruction of spring/summer precipitation from the lower Bavarian forest region, Germany. *Int. J. Climatol.* **25**, 611–630 (2005).
25. Tett, S. F. B. et al. The impact of natural and anthropogenic forcings on climate and hydrology since 1550. *Clim. Dyn.* (submitted).
26. Allen, M. R. & Ingram, W. J. Constraints on future changes in climate and the hydrological cycle. *Nature* **419**, 224–232 (2002).
27. Emori, S. & Brown, S. J. Dynamic and thermodynamic changes in mean and extreme precipitation under changed climate. *Geophys. Res. Lett.* **32**, 10.1029/2005GL023272 (2005).
28. Leavitt, S. W. & Long, A. Sampling strategy for stable isotope analysis of tree-rings in pine. *Nature* **311**, 145–147 (1984).
29. Wigley, T. M. L., Briffa, K. R. & Jones, P. D. On the average of correlated time series, with applications in dendroclimatology and hydrometeorology. *J. Clim. Appl. Meteorol.* **23**, 201–213 (1984).
30. Briffa, K. R. et al. Tree-ring width and density data around the Northern Hemisphere: Part 1, local and regional climate signals. *Holocene* **12**, 737–757 (2002).

**Supplementary Information** is linked to the online version of the paper at [www.nature.com/nature](http://www.nature.com/nature).

**Acknowledgements** We are grateful to K. Briffa, E. Cook, E. Hendy, R. Wilson, M. Gagen, J. Waterhouse, M. Gumpert and U. Büntgen for comments and suggestions. We thank S. Andres, B. Kammer, W. Laumer, G. Reiss, M. Schrimpf and C. Welscher for laboratory assistance, and C. Welscher, M. Gumpert and A. Shafgat for logistical support in the field. This research was funded by the German Federal Ministry for Education and Research, the German Science Foundation Schl 3-1, the European Union (ALPIMP and ISONET) and the Swiss National Science Foundation (NCCR-Climat).

**Author Information** Reprints and permissions information is available at [npg.nature.com/reprintsandpermissions](http://npg.nature.com/reprintsandpermissions). The authors declare no competing financial interests. Correspondence and requests for materials should be addressed to K.S.T. ([kerstin.treydte@wsl.ch](mailto:kerstin.treydte@wsl.ch)).

# Twentieth century as the wettest period in northern Pakistan over the past millennium

## Supplementary tables, figures, legends, notes and references

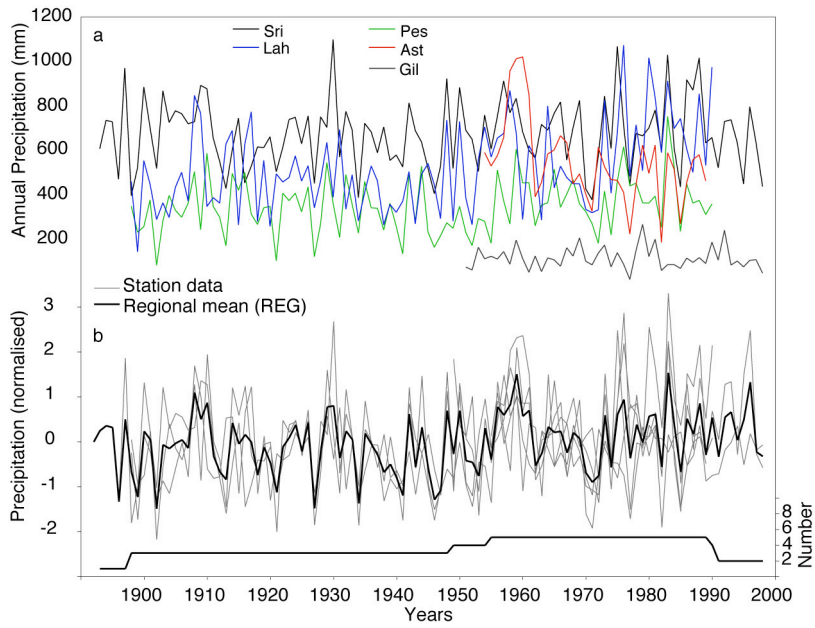
Site name	Coordinates	Altitude (m)	Exposure	Species	Number of trees/samples	Period
Ram-high	35°22'N 74°52'E	3600	S	<i>Juniperus turkestanica</i>	4/8	1900-1998
Bag-high	36°02'N 74°35'E	3800	S	<i>Juniperus turkestanica</i>	4/8	1900-1998
Bag-low	36°02'N 74°35'E	2900	S	<i>Juniperus excelsa</i>	5/10	1900-1998
Mor-high	36°35'N 75°05'E	3900	SE	<i>Juniperus turkestanica</i>	7/14	826-1998

**Supplementary Table 1:** Sampling site information

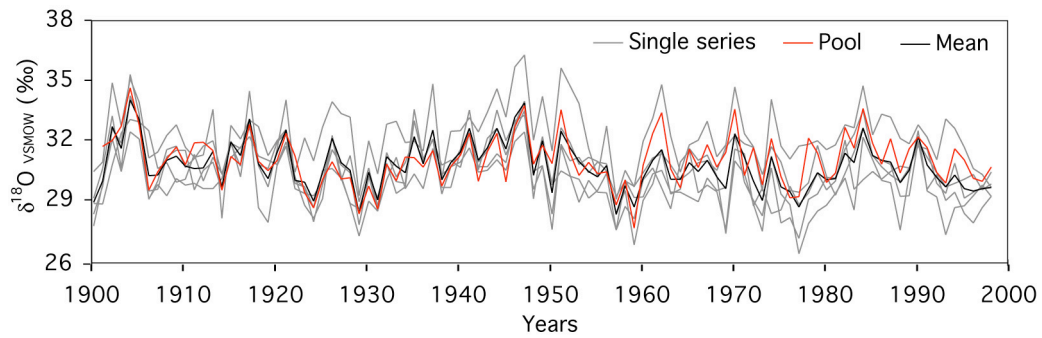
O-s	Sri	Pes	Lah	Ast	Gil
	Temperature				
Sri		<b>0.73</b>	<b>0.63</b>	<b>0.74</b>	<b>0.53</b>
Pes	<b>0.47</b>		<b>0.83</b>	<b>0.60</b>	<b>0.41</b>
Lah	<b>0.50</b>	<b>0.44</b>		<b>0.54</b>	0.29
Ast	<i>0.35</i>	0.25	0.07		<b>0.74</b>
Gil	<b>0.33</b>	0.27	0.08	0.27	
	Precipitation				

**Supplementary Table 2:** Inter-station correlations using annual (October-September, O-S) means of temperature (upper right) and normalized precipitation (lower left).

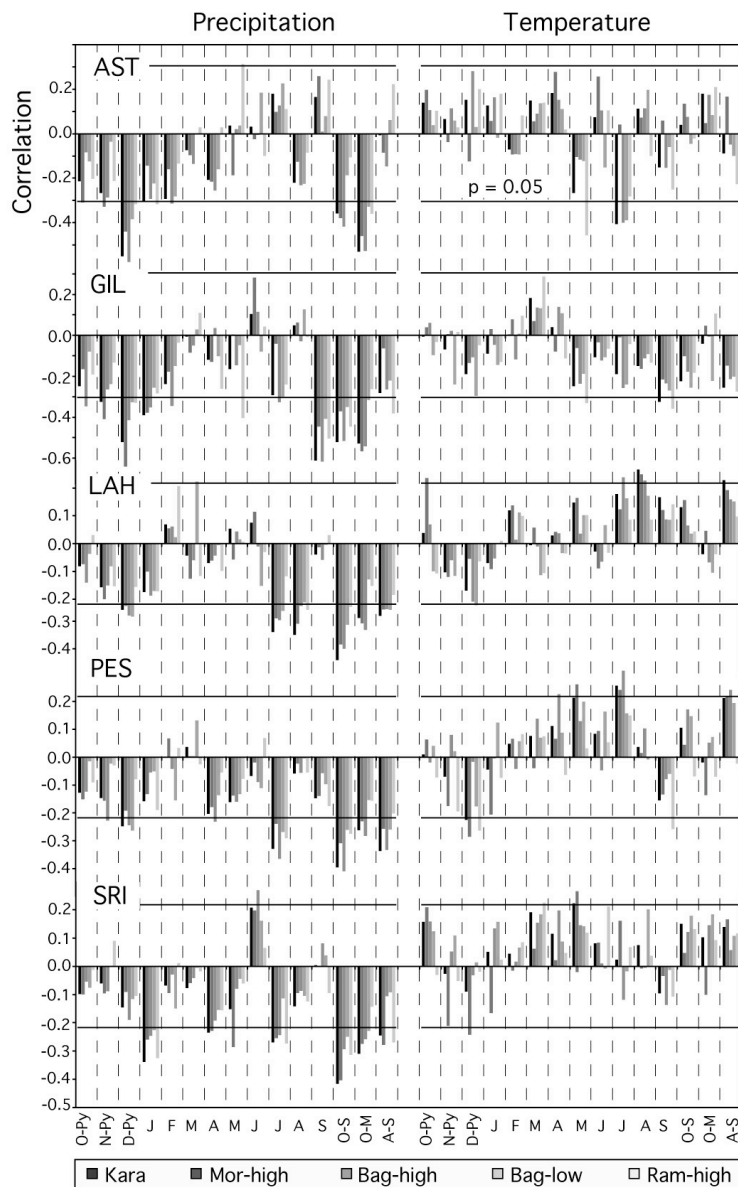
Correlations are based on the common period AD 1954-1989. SRI=Srinagar, PES=Peshawar, LAH=Lahore, AST=Astor, GIL=Gilgit. Bold:  $p < 0.05$ , italics:  $p < 0.01$ .



**Supplementary Figure 1:** Annual (October to September) precipitation data from Srinagar (SRI), Peshawar (PES), Lahore (LAH), Astore (AST) and Gilgit (GIL); **a** precipitation means; **b** data normalized over individual series lengths, the mean of these series and also the number of series contributing to the mean.

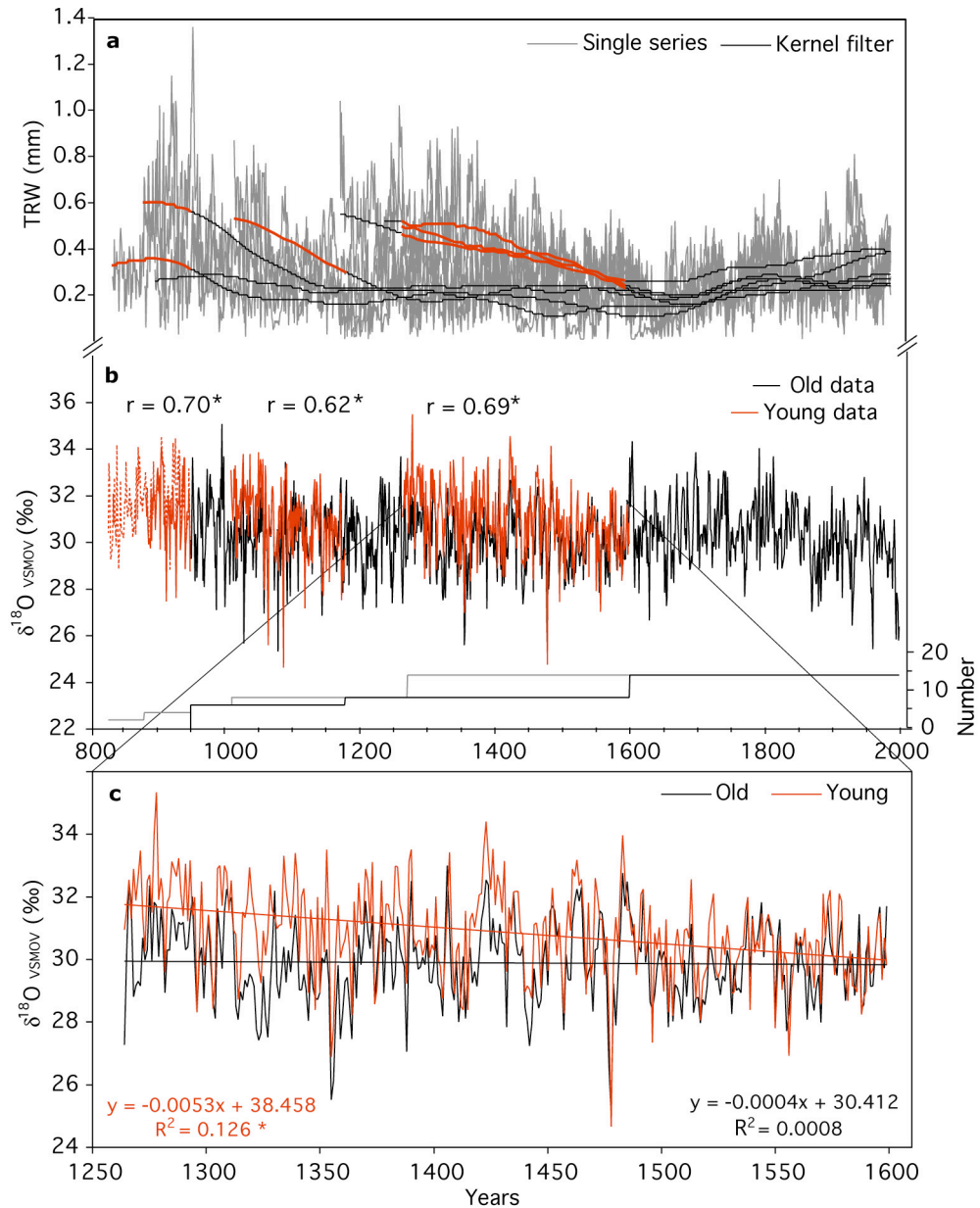


**Supplementary Figure 2:**  $\delta^{18}\text{O}$  measurements from five single trees at Bag-low, their arithmetic mean, and the  $\delta^{18}\text{O}$  curve obtained from pooling the rings of the same trees before single-series-measurements. The series are homoscedastic with no spread-versus-level relationship, as is generally the case with tree-ring width measurements<sup>1</sup>. The mean inter-series correlation of 0.62 is highly significant ( $p < 0.001$ ). The arithmetic mean of the five series (black) correlates at 0.85 with the pooled record (red), validating the pooling method.



**Supplementary Figure 3:** Correlations between tree-ring  $\delta^{18}\text{O}$  and normalized precipitation and temperature data for each of the five meteorological stations; correlation coefficients are shown for each of the four tree sites and their variance adjusted mean (Kara) from October of the previous year (Py) to September of the current year (O-S), winter half year (October-March, O-M) and summer half year (April-September, A-S). The climate signal, seen when calibrating against the regional mean series REG (Fig. 2b, main text) is supported by the results using single station data. AST and GIL are situated within the study region, and are most representative for the tree sites despite elevational differences of about 1000 m. Both validate the winter precipitation signal being dominant. LAH, PES and SRI highlight spring and summer

conditions also being of importance suggesting integration of whole year conditions. As discussed for REG, only weak and heterogenous correlations are found with summer temperature conditions.



**Supplementary Figure 4:** Potential age-related biases in ring-width and  $\delta^{18}\text{O}$  measurements. **a** Ring-widths of seven trees used for isotope analyses at Mor. 101-year smoothing Kernel filters indicate, that the early segments (red), showing systematically wider rings, are biased by age-related effects commonly known as age-trend. **b** Pooled

oxygen record (black) using cellulose from only “old” rings versus shorter segments (red) using only “young” rings. “r” is the correlation for the periods 881-950, 1077-1178, and 1264-1599. The record for the latter period is derived from pooling the three younger trees. Bottom: Numbers of samples combined in the long record using only the old (black) and all data (gray). **c** Least-square linear fits to the  $\delta^{18}\text{O}$  time-series from young and old data over the 1264-1599 period show that there is a significant long-term  $\delta^{18}\text{O}$  trend in the records containing juvenile rings but none over the same time period from records composed only of older rings.

#### **Notes to supplementary figure 4:**

Ring-width measurements from our 1000-year old living juniper trees (Mor) are strongly biased by non-climatic, age-related trends, commonly found in growth proxy data (ring-widths, wood density)<sup>1</sup>. In these junipers, the age-trend and long-term temperature changes tend to mimic each other during the cooling from the Medieval Warm Period (MWP) into the Little Ice Age (LIA)<sup>2,3</sup>, making unbiased estimates of past climate challenging. To date, such biases have not been reported for oxygen isotopes. We tested the age-level relationship in  $\delta^{18}\text{O}$  time-series over the past millennium using cellulose from “old” and narrow rings, and comparing this record with three shorter segments composed of “young” and wide rings (Supplementary Fig. 3b). These segments all correlate  $>0.62$  with the long record, thus demonstrating a common signal in the mid-to-higher frequencies. However, linear fits to the young and old data over the 1264-1599 period, during which the growth rate differences between both are maximum, indicate a significant trend ( $p < 0.001$ ) for the time-series from young rings but no trend from the old rings (Supplementary Fig. 3c).

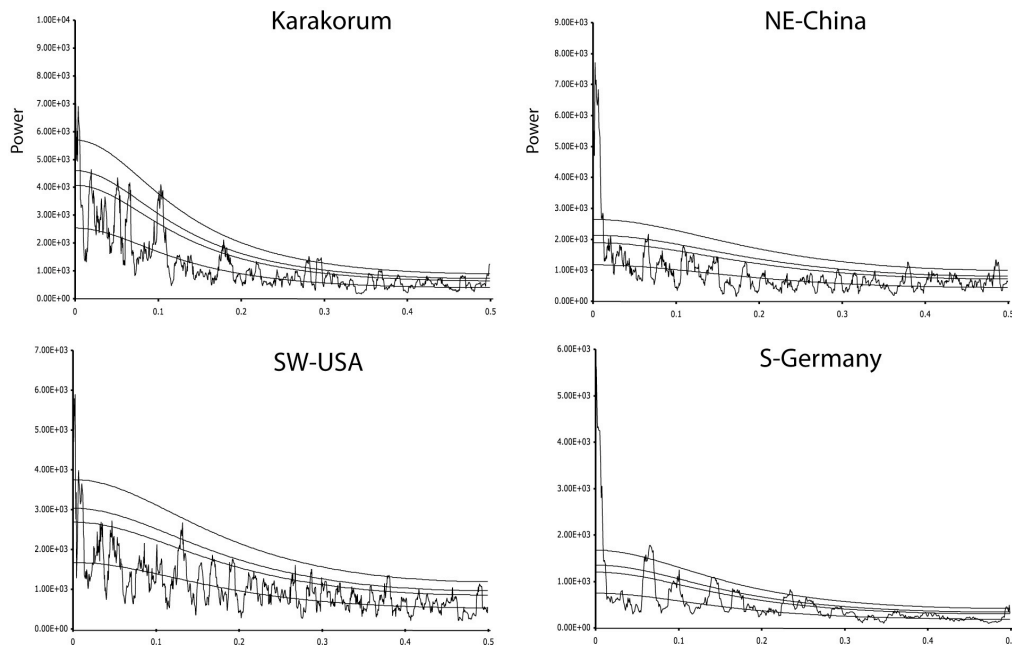
For the first time, these results suggest that long-term age-related effects could exist in  $\delta^{18}\text{O}$  measurements. Several factors could account for the observed age-related

$\delta^{18}\text{O}$  decrease found in young juniper trees. Based on tree physiological considerations, we here present two possible explanations.

(i)  $\delta^{18}\text{O}$  variations in up-taken water are the baseline for variations in tree ring cellulose. Although young and old trees originate from the same site, they might access different source water. Because of a their shallow root system, young trees take up relatively more of water from the upper soil. Due to evaporative effects, this water has up to 6‰ higher  $\delta^{18}\text{O}$  values than water deeper in the soil<sup>4, 5</sup>.

(ii) The differences in  $\delta^{18}\text{O}$  of tree ring cellulose between young and old trees might additionally be caused by differences in  $^{18}\text{O}$  enrichment of leaf water. Evapotranspiration enriches leaf water because the heavier  $\text{H}_2^{18}\text{O}$  vapour has a lower vapour pressure than  $\text{H}_2^{16}\text{O}$ , and  $\text{H}_2^{18}\text{O}$  diffuses more slowly than  $\text{H}_2^{16}\text{O}$ . The extent of  $^{18}\text{O}$  enrichment depends on the leaf-to-air water vapor pressure gradient. Trees grown in humid conditions show generally lower  $\delta^{18}\text{O}$  values than those grown in dry conditions<sup>6</sup>. In the open juniper stands, considered here, air humidity can assumed to be the same for young and old trees. However, a less developed root system with slightly inferior water supply could lead to a higher leaf-to-air water vapor pressure gradient with higher  $^{18}\text{O}$  enrichment in young trees as compared to old trees.

The presence of age-related  $\delta^{18}\text{O}$  trends would have significant implications for preserving long-term variability in the millennium-long chronology and more generally for all  $\delta^{18}\text{O}$  tree-ring applications. Hence, in the main paper we show the long reconstruction using all tree-ring data together with results obtained by excluding young-ring cellulose (fig. 3b, main text).



**Supplementary Figure 5:** Power spectra (multitaper method<sup>7</sup>) of the four annually resolved precipitation reconstructions shown in fig. 4 of the paper. Smoothed curves are 50%, 90%, 95% and 99% red noise significance levels. All spectra tend to be consistent towards the red noise component with substantially more variance in the decadal to centennial time scales than at higher frequencies.

## References

1. Fritts, H. C. *Tree-rings and climate*. (Academic Press, London, 1976).
2. Esper, J., Schweingruber, F. H. & Winiger, M. 1,300 years climate history for Western Central Asia inferred from tree-rings. *The Holocene* **12**, 267-277 (2002).
3. Esper, J. et al. Temperature-sensitive Tien Shan tree-ring chronologies show multi-centennial growth trends. *Clim. Dyn.* **21**, 699-706 (2003).

4. Drake, P. L. & Franks, P. J. Water resource partitioning, stem xylem hydraulic properties, and plant water use strategies in a seasonally dry riparian tropical rainforest. *Oecologia* **137**, 321-329 (2003).
5. Hsieh, J. C. C., Chadwick, O. A., Kelly, E. F. & Savin, S. M. Measurement of soil-water  $^{18}\text{O}$  by in situ  $\text{CO}_2$  equilibration Method. *Geoderma* **82**, 255-269 (1998).
6. Roden, J.S., Lin, G.G. & Ehleringer, J.R. A mechanistic model for interpretation of hydrogen and oxygen isotope ratios in tree-ring cellulose. *Geochim. Cosmochim. Acta* **64**, 21-35 (2000).
7. Mann, M. E., Lees, J. M. Robust estimation of background noise and signal detection in climate time series. *Climatic Change* **33**, 405-445 (1996).